An Adaptive Chebyshev Approach for Fast Computation of Grounding System Admittance Matrix

Valiollah Mashayekhi, Seyed Hossein Hesamedin Sadeghi, *Senior Member, IEEE*, Rouzbeh Moini, *Senior Member, IEEE*, and Keyhan Sheshyekani, *Senior Member, IEEE*

***Abstract*—The paper proposes an adaptive Chebyshev method for expediting the calculation of grounding system admittance matrix. This facilitates the characterization and the inclusion of the wideband model of the grounding systems into the time-domain electromagnetic transient solvers. In the proposed method, a general electromagnetic approach based on the method of moments (MoM) solution to Maxwell's equations is utilized to obtain the grounding system admittance matrix over the frequency range of interest. Rather than applying the MoM to each distinct frequency obtained from the FFT procedure, the proposed method is utilized to reduce the number of frequency points for which the response of grounding system is calculated. Several simulated case studies are presented to examine the accuracy of the proposed method. It is shown that the selected sampling frequencies are sufficient to generate the exact response of the grounding system over the working frequency interval**

***Index Terms*—Chebyshev functions, grounding, lightning, state space methods.**

I. Introduction

THE inclusion of grounding system wideband model into the electromagnetic transient solvers has attracted a great deal of attention in recent years [1]–[4]. The relevance is mainly due to the need for accurate calculation of lightning generated overvoltages within the electrical networks.

As known, lightning impulse currents are characterized by their wide frequency content in the range of zero to several MHz over which the grounding system impedance varies as a function of frequency. Various methods have been proposed in the literature to implement the grounding system exact model in the electromagnetic transient tools among which the approach presented in [1] and [2] seems to be more general and comprehensive. In this approach, the grounding system admittance matrix seen from different ports is to be accurately calculated over the working frequency interval. To this aim, the governing Maxwell's equations are solved by making use of rigorous numerical methods such as the method of moments (MoM).

The application of numerical methods in the analysis of grounding system, in particular for large grounding grids, is, however, brute forcing and requires a huge computation time. This is a key issue for optimal design [5] and statistical human safety risk assessment of grounding systems [6]. Also, the inclusion of grounding system exact model into the electromagnetic transient program (EMTP)-like tools is not practical unless the calculation of the grounding system admittance matrix becomes sufficiently fast. This is important in the sense that the next versions of EMTP-like tools are expected to add the grounding system calculation module to their software packages.

Within the context alluded earlier and as a continuation of the concept developed in [1], this paper proposes an adaptive Chebyshev method for expediting the calculation of grounding system admittance matrix. In the proposed method, a general electromagnetic approach based on the MoM solution of Maxwell's equations is utilized to obtain the grounding system admittance matrix over the frequency range of interest. This is done by applying the method of moments to the electric field integral equation (EFIE) governing the electromagnetic behavior of the current-carrying grounding conductors. To decrease the computation time, due to the time-consuming nature of the solution in the frequency domain, an adaptive Chebyshev method is utilized to reduce the number of frequency points. This can remarkably decrease the time required for the calculation of the grounding system admittance matrix.

To demonstrate the application of the proposed method in a practical setting, we study the effect of wide band modeling of grounding system on the transient behavior of a wind-turbine generation system.

The rest of the paper is organized as follows. In Section II, the Chebychev interpolation method is discussed, while the electromagnetic modeling of the grounding systems and its MoM solution are briefly revisited in Section III. A cursory review for the pole–residue identification of the grounding system admittance matrix by making use of the matrix pencil method (MPM) and its state-space representation is provided in Section IV. Numerical results and the validation of the proposed method are discussed in Section V.

II. Chebyshev Interpolation Method

In this section, we present a one-stage adaptive method for interpolating the grounding system impedance matrix. The

Manuscript received February 9, 2016; revised May 24, 2016 and July 12, 2016; accepted August 21, 2016.

V. Mashayekhi, R. Moini, and S. H. H. Sadeghi are with the Department of Electrical Engineering, Amirkabir University of Technology, Tehran 1591634311, Tehran (e-mail: vali_mash@yahoo.com; rouzbeh.moini@gmail.com; sadeghi@aut.ac.ir).

K. Sheshyekani was with the Department of Electrical and Computer Engineering, Shahid Beheshti University, Tehran 1983969411, Tehran. He is now with the Department of Electrical Engineering, Polytechnique Montréal, Montreal, QC H3T 1J4, Canada (e-mail: k_sheshyekani@sbu.ac.ir).

Color versions of one or more of the figures in this paper are available online at http://ieeexplore.ieee.org.

Digital Object Identifier 10.1109/TEMC.2016.2611675

method will be used to speed up the MoM solution of the governing Maxwell's equations for obtaining the grounding system admittance matrix over the frequency range of interest (i.e., $f_0 \leq f \leq f_1$).

Knowing that the functional behavior of grounding system harmonic impedance is continuous and sufficiently smooth over the range of lightning frequency components [3], one can expand it in terms of Chebyshev orthogonal basis functions as follows [7], [8]:

$$Z(f') \cong P(f') = \lim_{N\to\infty} P_N(f') = \lim_{N\to\infty} \sum_{n=0}^{N} a_n T_n(f') \quad (1)$$

where $f' = (2f - f_1 - f_0)/(f_1 - f_0)$ is the mapped frequency to $[-1,\ 1]$, a_n $(n = 0,\ \ldots N)$ are the unknown coefficients to be determined, $T_n(f')$ is the first-kind Chebyshev basis function of order n, and f' represents the frequency of interest.

By sampling $P(f')$ at total of $(N+1)$ frequencies f'_n $(n = 0,\ \ldots, N)$, (1) can be written as an $(N+1) \times (N+1)$ matrix equation with the form

$$AX = b \quad (2)$$

where

$$X = [a_0 \quad a_1 \quad \ldots \quad a_N]^T \quad (3)$$

and

$$A = \begin{bmatrix} T_0(f'_0) & T_1(f'_0) & \cdots & T_N(f'_0) \\ T_0(f'_1) & T_1(f'_1) & \cdots & T_N(f'_1) \\ \vdots & \vdots & \vdots & \vdots \\ T_0(f'_N) & T_1(f'_N) & \cdots & T_N(f'_N) \end{bmatrix} \quad (4)$$

$$b = \begin{bmatrix} Z(f'_0) & Z(f'_1) & \cdots & Z(f'_N) \end{bmatrix}^T. \quad (5)$$

Equation (2) can be solved to determine the unknown coefficients x using the well-known numerical techniques such as the single value decomposition, LU decomposition, or iterative solution techniques [9].

The main idea is to employ an adaptive method to calculate as minimum number of a_n as possible while preserving $|Z(f') - P_N(f')| < \epsilon$, where $P(f')$ has $(N+1)$ unknown complex coefficients. A flowchart of the algorithm is shown in Fig. 1. With reference to this figure, the first $P_1(f')$ and the second $P_2(f')$ versions of $P(f')$ are formed in the beginning of the algorithm; $P_1(f')$ is determined using the first and the last points of the interval $[-1,\ 1]$, while $P_1(f')$ is constructed using the aforementioned points as well as the midpoint of the interval $(f' = 0)$. The algorithm will then enter an iterative procedure, starting with a quality check. The basic requirement of such an adaptive model is a suitable error function. When dealing with impedance or admittance matrices, we must be able to interpolate all element of the matrix simultaneously for same sampling points to minimize the computational time. The error function must encompass all elements of the matrices. The error function

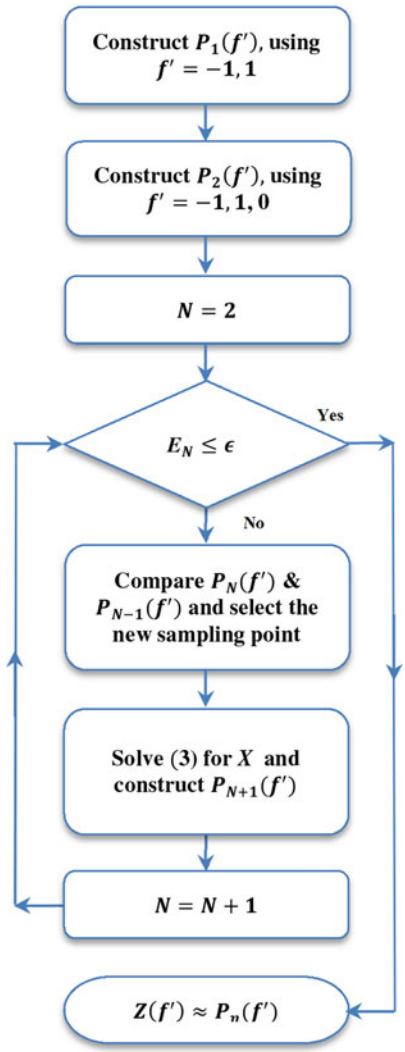

Fig. 1. Flowchart of the proposed algorithm.

at iteration N can be expressed as

$$E_N = \left\| \sum_{m=1}^{M} \frac{\left|P_N^m(f') - P_{N-1}^m(f')\right|^2}{1 + \left|P_N^m(f')\right|^2} \right\| \quad (6)$$

where $\|\cdot\|$ denotes the 2-norm operator, M represents the number of interpolated objects, and $P_N^m(f)$ is the Nth degree of the mth interpolated object.

Provided that E_N is less than a prespecified value ϵ, the algorithm stops. Otherwise, the absolute errors between various points within the interval associated with the last two consecutive versions of $P(f')$ are calculated and a new sampling point is selected at the checkpoint where the maximum absolute error occurs. The new point will be used to form the next updated $P(f')$. This is done by first determining the closest point in the Chebyshev–Gauss–Lobatto (CGL) quadrature sampling set [10]. It is noted that for a given value of N, the CGL quadrature provides a set of interpolating points x_n

$$x_n = -\cos\left(\frac{\pi n}{N}\right) \qquad (n = 0 : N) \quad (7)$$

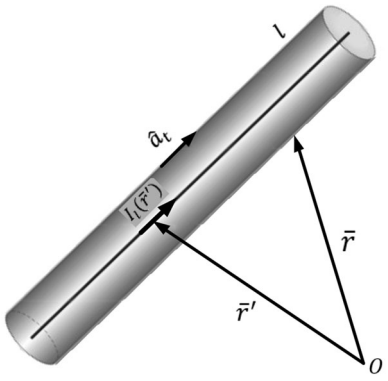

Fig. 2. Thin-wire approximation for ground conductors.

that minimizes the error function.

Having found the appropriate CGL point, the new augmented sampling set is used to update $P(f')$ for the next iteration (see Fig. 1). When calculating the error function, the CGL point is not included in (6) to avoid unnecessary increase of E. This is due to the fact that $P_N(f')$ is not necessarily required to pass the last sampling point $(f'_{N+1},\ Z(f'_{N+1}))$.

It is worth noting that since the original function is sufficiently smooth, the final interpolated function converges to the original function according to the Weiestrass approximation theory [11], eliminating the need for comparison with the original model.

III. Electromagnetic Model of Grounding System

For operational and safety reasons, various apparatus in a typical power plant are connected to the grounding system, forming a multiport network [12]. Such a linear network can be represented by an impedance matrix. To obtain the impedance matrix over the frequency range of interest, we start by adopting the thin-wire approximation for representing the ground conductors, as shown in Fig. 2.

Referring to Fig. 2, the total electric field $E^t(r)$ at an arbitrary point point $\bar{r}$ is the sum of the incident $E^i(\bar{r})$ and scattered $E^s(\bar{r})$ fields, i.e.

$$E^t(\bar{r}) = E^i(\bar{r}) + E^s(\bar{r}). \tag{8}$$

Considering the vanishing condition for the tangential component of the electric field at the surface of the conductor and applying it to the governing EFIE, we have [13]

$$\hat{a}_t . E^i(\bar{r}) = \frac{j\omega\mu}{4\pi} \int_l I_l\left(\overline{r'}\right) G(\bar{r}, \bar{r}')\, dl \tag{9}$$

where $\hat{a}_t$ is the unit vector tangential to the ground conductor path, $I_l(\bar{r}')$ is the unknown longitudinal current along the ground conductor, and $G(\bar{r}, \bar{r}')$ is the dyadic Green's function for the electric field at point $\bar{r}$ due to a current element at point $\bar{r}'$.

By making use of the MoM, (9) can be solved for $I_l(\overline{r'})$ [2], [13]. Having obtained the current distribution along the ground conductors, one can obtain the values of the voltage and current at the ports to form the system impedance matrix in the frequency domain. It is worth noting that the matrix elements are functions of the geometry of the grounding system as well as the soil electrical properties.

IV. Matrix Pencil Method

To obtain the rational approximation of frequency domain responses, we adopt the customized MPM described in [14]. In this section, the method is summarized for the case of grounding system admittance matrix.

Let $y(t)$ represents the time domain representation of the admittance frequency domain response of an arbitrary port of a grounding system. The MPM is used to approximate .. as a sum of exponentials (SoE) [14]–[16]

$$y(t) = \sum_{i=1}^{M} R_i e^{P_i t} \tag{10}$$

where P_i $(i = 1 : M)$ are the complex valued poles of the system, R_i stands for residue, and M is the number of poles. The rational form of (10) can be derived as follows (11):

$$Y(s) = \sum_{i=1}^{M} \frac{R_i}{s - P_i} \tag{11}$$

where Y denotes the Laplace transform of $y(t)$ and s is the complex frequency,

For considering the mutual impedances between different ports, all the elements of the grounding system admittance matrix are stacked into a single vector, which is fitted by the MPM generating a common set of poles (P_i) for each individual element. A least square problem is solved to calculate the individual residues (R_i) [15].

The grounding systems characterized in this paper constitute an *n*-port linear time-invariant (LTI) system. The requirements for physically consistent modeling for LTI systems are stability, causality and passivity [16]. In the frequency domain, the stability of the system is guaranteed when the poles of the system lie in the left-hand side of the imaginary axis (i.e., poles with negative real parts) [16], [17].

The grounding system model is passive if and only if its admittance matrix transfer function is positive real [18]. This requires the following:

1) The admittance matrix transfer functions have no poles with positive real parts.
2) All eigenvalues of real part *G* of *Y* matrix be positive [19], [20].

After obtaining a passive pole–residue representation for the frequency response of each element of the admittance matrix, a time-domain representation the admittance matrix is needed to include the frequency response of the grounding system in EMTP-RV. The state space equations are formulated as follows [21]:

$$\begin{aligned} \dot{x}(t) =&\ A \cdot x(t) + B \cdot v(t) \\ i(t) =&\ C \cdot x(t) + D \cdot v(t) + E \cdot \dot{v}(t) \\ A \in&\ R^{m\times m}, B \in R^{m\times n}, C \in R^{n\times m}, \\ & D \in R^{n\times n}, E \in R^{n\times n} \end{aligned} \tag{12}$$

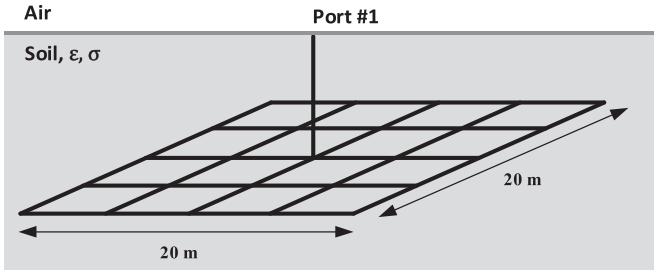

Fig. 3. Schematic of a 20×20 m^2 grounding grid with 4×4 meshes.

where $x(t)$ is the sate vector, n denotes the number of system ports, and m is the total number of state variables, which equals the product of the total number of the poles and the total number of the ports $(m = M \times n)$.

The Jordan-canonical form is chosen for time-domain realizations for the fitted admittance matrix in the form of state space equation. The obtained state-space equations can be directly implemented in EMTP-RV using the state space block [21].

V. Results

In order to demonstrate the efficiency of the proposed method, three different grounding systems are studied. To this aim, both single-port and multiport grounding systems are considered. To evaluate the effect of wideband modeling of grounding systems on the lightning generated overvoltages, the proposed method will be used in conjunction with the EMTP-RV simulator for analyzing a typical wind power plant.

In all simulations presented in this section, we assume that the grounding electrodes are assumed to be perfect electric conductor which is a reasonable approximation for the working frequencies [22]. Also, the soil is assumed to be single layer characterized by relative permittivity of $\varepsilon_r = 20$ and conductivity of $\sigma_0 = 0.001$ S/m. The simulations are carried out on an Intel Quad core, 3632 QM at 2.2 GHz, with 6 GB of RAM.

A. One-Port Grounding Grid

First, we consider the case of a single-port grounding grid buried in a single layer lossy soil, as shown in Fig. 3. The grounding grid in this case is an equally spaced 20×20 m^2 square with 4×4 meshes. The burial depth of the grid is $h = 1$ m, and the conductors have a radius of $r = 15$ mm.

Variations of the magnitude and phase of the harmonic impedances of the grounding grid are shown in Fig. 4. The harmonic impedance of the grounding grid was fitted by the proposed method over the frequency range of $0 - 3$ MHz. It is found that only six sampling points $(f = 0.1, 262, 976, 1500, 2405,$ and 3000 kHz). are required to achieve a relative error of $E = 0.05$. The computational time decreases from 350 s for conventional method approach to about 15 s for the proposed method.

From this, it is clear that the Chebychev method can result in a significant reduction in the computation time with respect to the conventional method with the same desired accuracy.

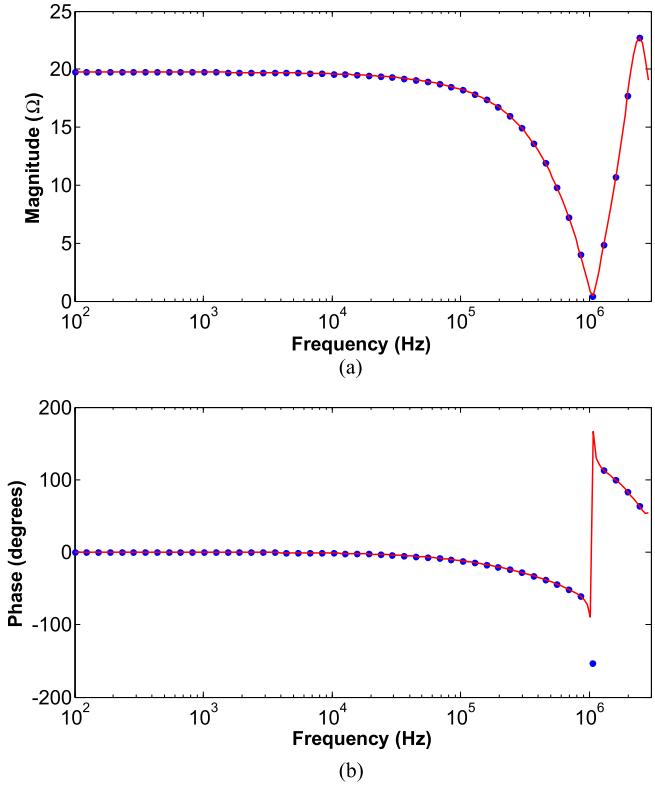

Fig. 4. (a) Magnitude and (b) phase variations of the harmonic impedances of the single-port grounding grid shown in Fig. 3; solid line indicates the conventional method with $N = 256$ and dotted line indicates the proposed method with $N = 6$.

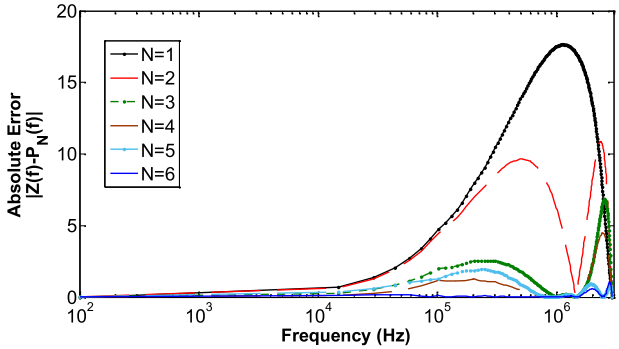

Fig. 5. Progression of the absolute error $(|Z(f) - P_N(f)|)$ of the computed impedance of the single-port grounding system (see Fig. 3) as a function of frequency.

As discussed earlier in this paper, it is important when the admittance matrix of a large grounding system is intended to be implemented in the time-domain EMTP-like tools.

To demonstrate the convergence rate of the proposed method, the absolute error between the original model $Z(f)$ and the interpolated models $P_N(f)$ $(N = 1 : 6)$ in various iterations are presented in Fig. 5. A study of the results in this figure clearly shows the convergence of the proposed method.

B. Two-Port Grounding Grid

To further demonstrate the ability of the proposed method, we consider a 60×60 m^2 two-port grounding grid, as shown in

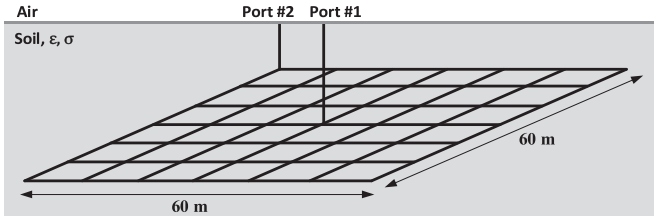

Fig. 6. Schematic of a two-port $60 \times 60\ \mathrm{m}^2$ grounding grid with 6×6 meshes.

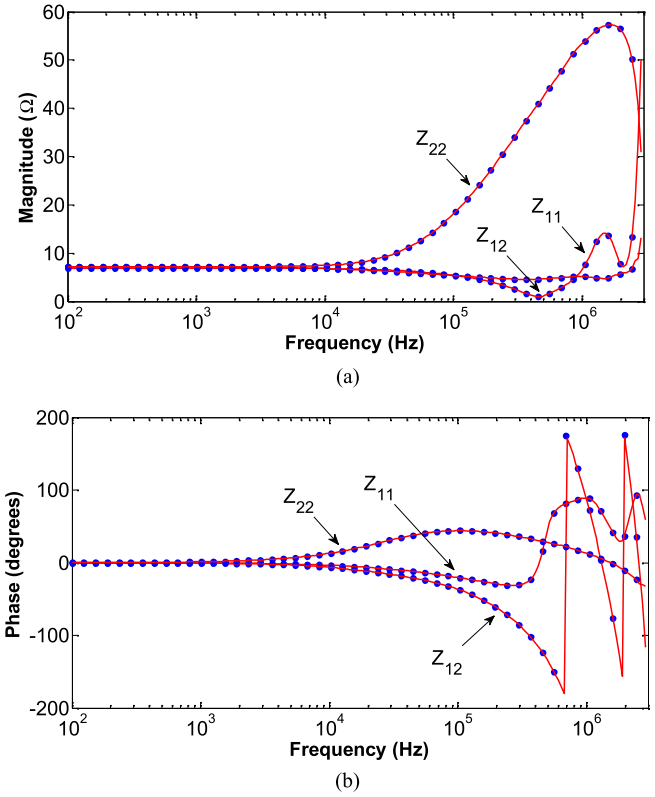

Fig. 7. (a) Magnitude and (b) phase variations of the self (Z_{11} and Z_{22}) and mutual ($Z_{12} = Z_{21}$) harmonic impedances of the two-port grounding grid shown in Fig. 6; solid line indicates the conventional method with $N = 256$ and dotted line indicates the proposed method with $N = 7$.

Fig. 6. The grid in this case study consists of 6×6 equally spaced square meshes with two ports located at the corner and the center of the grid. The grid is buried at the depth of $h = 0.5$ m, and the conductors are of radius of $r = 15$ mm. The soil electrical parameters are identical to the previous case. Calculating the self- and mutual impedances of the grounding system results in a 2×2 impedance matrix whose off-diagonal elements (Z_{12} and Z_{21}) are equal due to the reciprocity.

Variations of the magnitude and phase of the self (Z_{11} and Z_{22}) and mutual ($Z_{12} = Z_{21}$) harmonic impedances of the two-port grounding system are shown in Fig. 7. As it can be seen in this figure, the proposed method can accurately ($E = 0.08$)reconstruct the self- and mutual impedances using only seven frequencies ($f = 0.1,\ 455, 656, 1500, 1997, 2682$ and 3000 kHz) within the working frequency interval.

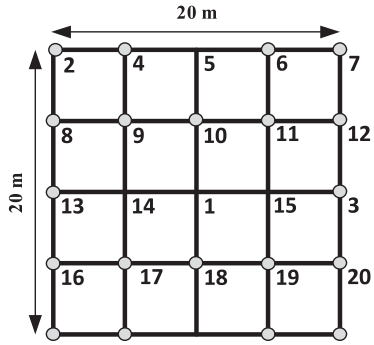

Fig. 8. Port numbering in the $20 \times 20\ \mathrm{m}^2$ grounding grid shown in Fig. 3.

TABLE I
TOTAL COMPUTATION TIMES OF THE SELF- AND MUTUAL IMPEDANCES OF THE MULTIPLE PORT GROUNDING SYSTEMS SPECIFIED IN FIGS. 3 AND 8, WITH RELATIVE ERROR OF $E \leq 0.05$

		Computation Time (s)	
No. of Ports	No. of Sampling Points	Proposed Method	Conventional Method
2	7	32	706
4	8	73	1413
6	8	109	2119
8	8	145	2826
10	8	182	3532
12	8	218	4239
14	8	254	4945
16	8	290	5652
18	8	327	6359
20	9	407	7065

It is worth noting that the same sampling points are used to fit all three self- and mutual harmonic impedances. Reducing the number of sampling points from 256 to 7 substantially enhances the efficiency of the computations. In fact, the computation time decreases by a factor of 20 from 700 s to about 30 s.

C. Multiport Grounding Grid

To demonstrate how the proposed method can affect the computation time in the analysis of a complex multiport grounding system, we consider the same $20 \times 20\ \mathrm{m}^2$ grounding grid with several ports, as shown in Fig. 8. The analysis is repeated for various case studies involving $2, 4, \ldots 20$ ports. The results are shown in Table I where the computation times of the proposed method for determining the self- and mutual impedances are compared with those obtained using the conventional method. A study of the results in this table clearly confirms the efficiency of the proposed method. In fact, the computation gain increases as the number of ports increases. For example, the computation time difference between the two methods for the 2-port case is 674 s, whereas the proposed method requires 6658 s less time to determine the self- and mutual impedances of the 20-port grounding system. This is mainly due to the fact that as the number of ports increases, the number of self- and mutual impedances also increases while the reduced number

TABLE II
GRADE AND SPREAD VALUES COMPUTED FOR HARMONIC IMPEDANCES OF FIGS. 4 AND 7

Harmonic impedance	$\mathrm{GRADE_{ADM}}$	$\mathrm{SPREAD_{ADM}}$	$\mathrm{SPREAD_{FDM}}$	$\mathrm{GRADE_{FDM}}$
Z (see Fig. 4)	1	1	2	3
Z_{11} (see Fig. 7)	1	1	2	2
Z_{12} (see Fig. 7)	2	2	3	3
Z_{22} (see Fig. 7)	1	1	2	2

TABLE III
COEFFICIENTS α_i IN SMITH AND LONGMIRE MODEL FOR FREQUENCY DEPENDENCE OF SOIL ELECTRICAL PARAMETERS [27]

i	α_i	i	α_i
1	3.4×10^6	8	1.25×10^1
2	2.74×10^5	9	4.8×10^0
3	2.58×10^4	10	2.17×10^0
4	3.38×10^3	11	9.8×10^{-1}
5	5.26×10^2	12	3.92×10^{-1}
6	1.33×10^2	13	1.73×10^{-1}
7	2.72×10^1		

of frequency points required in the proposed method is almost unchanged for various number of ports.

To evaluate how closely the conventional method and the proposed method align, the feature selective validation (FSV) technique [23]–[25] is adopted; it is a simple and standard scheme for evaluating the reliability and quality of the comparison of two datasets. Among various figures of merit that the FSV technique offers, the amplitude difference measure (ADM) and feature difference measure (FDM) are used more commonly. They are based on the decomposition of the original data into "high" and "low" portions. Combinations of these portions of datasets and their derivatives are used to compute ADM and FDM [24], [25]. Having computed ADM and FDM, two quality factors, namely, GRADE and SPREAD, are presented for evaluating the quality of comparisons. The smaller the values of GRADE and SPREAD, the better the comparison. The GRADE and SPREAD values ranges from 1 (best quality) to 6 (worst quality).

The GRADE and SPREAD values of ADM and FDM are computed for the self- and mutual harmonic impedances shown in Figs. 4 and 7, respectively. A study of the results listed in Table II confirms that the proposed method can reliably reconstruct the harmonic impedances with a reduced number of frequency points.

D. Calculation of Overvoltages

To demonstrate the suitability of the proposed method for inclusion in the EMTP-RV simulator, the wideband modeling of the grounding system of a typical wind-turbine generation system on the lightning-generated overvoltages is studied. The grounding system admittance matrix is obtained using the method described in Sections II and III, while the pole–residue identification and hence the state-space model of the considered system are obtained by the procedure described in Section IV.

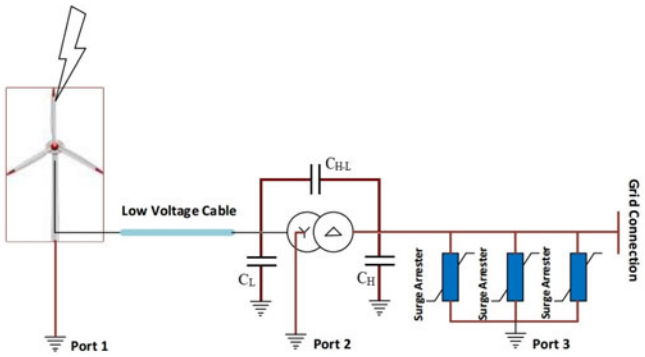

Fig. 9. Schematic of a single wind turbine power plant hit by lightning.

Measurements and simulations have shown that the frequency dependence of soil electrical parameters have considerable effects on grounding system impedances and the consequent transient voltages [26]. The analytical formulae, given later, proposed by Smith and Longmire [27] with a relative permittivity of $\varepsilon_\infty = 20$ and conductivity of $\sigma_{\mathrm{dc}} = 0.001$ S/m are used in this analysis

$$\varepsilon_r(f) = \varepsilon_\infty + \sum_{i=1}^{13} \frac{\alpha_i}{1 + \left(\frac{f}{F_i}\right)^2} \tag{13a}$$

$$\sigma(f) = \sigma_{\mathrm{dc}} + 2\pi\varepsilon_0 \sum_{i=1}^{13} \alpha_i F_i \frac{\left(\frac{f}{F_i}\right)^2}{1 + \left(\frac{f}{F_i}\right)^2} \left[\frac{\mathrm{S}}{\mathrm{m}}\right] \tag{13b}$$

where $F_i = (125\sigma_{\mathrm{DC}})^{0.8312} \times 10^{i-1}$ and α_i are given in Table III.

The plant consists of a wind turbine, a power transformer, and surge arresters, as shown in Fig. 9. The wind turbine encompasses a $2\,MW/690$ V synchronous generator with blade down conductors and tower lengths of 57 and 124 m, respectively. The blade down conductors and tower are modeled as constant parameter (CP) transmission lines characterized by surge impedances of 684 and 322 Ω, respectively [28], [29]. The values of the surge impedances are calculated based on the simple models developed for transmission lines with cylindrical geometry [30]. The tower is connected to the transformer via a short cable of length 50 m, which is modeled as a CP transmission line in EMTP-RV having a characteristic impedance of 50 Ω. The wind turbine generator is connected to a 20 kV distribution line via a 0.69 kV/20 kV ynD transformer with 2.5 MVA rated power. To model the ZnO surge arrester, the method described in [31] is used. The tower footing, the neutral point of the transformer, and the arresters are connected to the grounding system. To avoid computation of the complex transformer admittance matrix encountered in the wideband modeling, we adopt the π-capacitance model that consists of the transformer steady-state model together with high-frequency coupling capacitances [32], [33]. The values of the capacitance between the MV terminals and ground are obtained from manufacturer's data sheet. Referring to Fig. 9, they are $C_{\mathrm{H}} = 0.695$ nF, $C_{\mathrm{L}} = 0.455$ nF, and

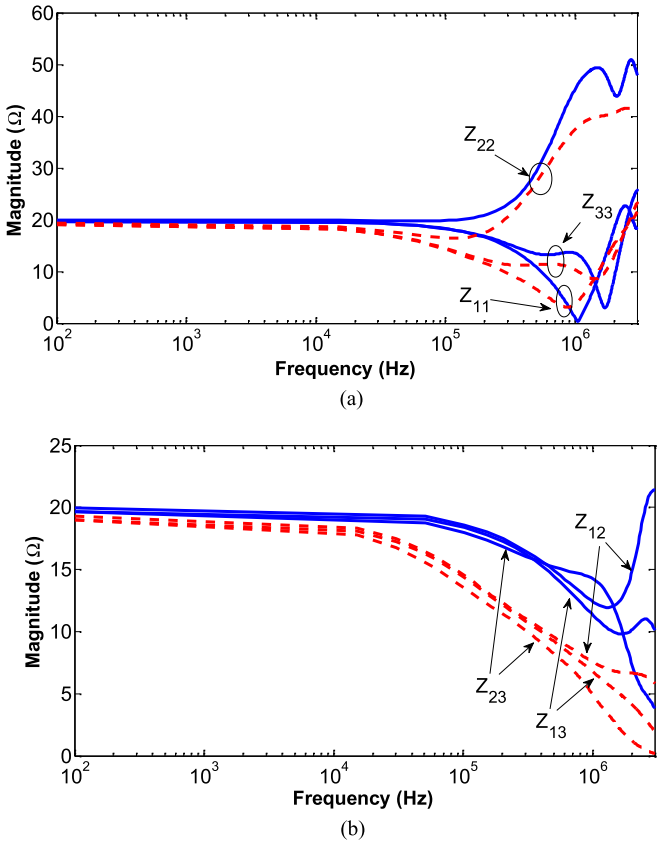

Fig. 10. Variations of the magnitudes of (a) the self- (Z_{11}, Z_{22} and Z_{33}) and (b) mutual (Z_{12}, Z_{13} and Z_{23}) harmonic impedances of the three-port grounding grid shown in Fig. 3; solid line indicates soil with CPs and dashed line indicates soil with frequency-dependent parameters.

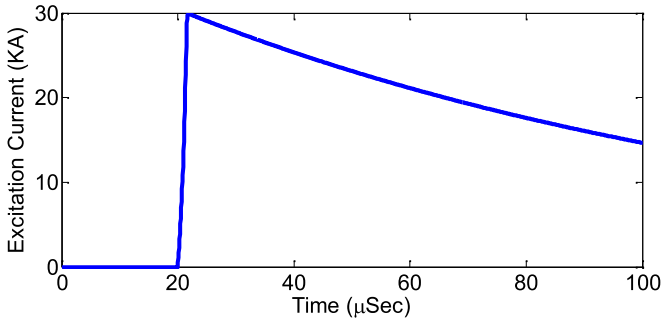

Fig. 11. Excitation current wave form with a rise time of $1.2\,\mu$s and a fall time of $77.5\,\mu$s having a peak current of 30 kA.

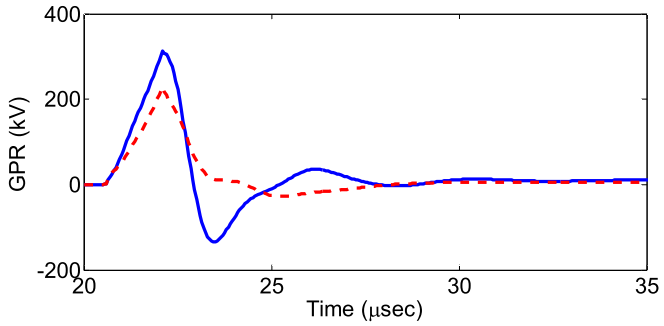

Fig. 12. Ground potential rise (GPR) at the wind turbine footing; solid line indicates soil with CPs and dashed line indicates soil with frequency-dependent soil parameters.

$C_{\mathrm{H-L}} = 0.235\,\mathrm{nF}$. It has been that the use of the π-capacitance model can provide a quite good estimation of transient voltages transferred from the transformer LV side to its MV side [32].

The grounding system is the three-port $20 \times 20\ \mathrm{m}^2$ grounding grid specified in Fig. 3 with ports 1, 2, and 3 shown in Fig. 8. To accurately fit the self- and mutual harmonic impedances ($E = 0.07$), the proposed method required only eight sampling points ($f = 0.1, 131, 597, 1020, 1500, 1720, 2463,$ and 3000 kHz) with a computation time of 48 s.

To illustrate the effect of the frequency dependence of the soil electrical parameters on the grounding system impedances, the magnitudes of the self- and mutual harmonic impedances for both constant and frequency-dependent soil electrical parameters are shown in Fig. 10. As it can be seen in this figure, the harmonic impedances, for both soils with constant and frequency-dependent parameters, take different values over the working frequency interval. As expected and in compliance with [3], [34], the frequency dependence of soil electrical parameters beneficially reduces the amplitude of the grounding system impedances

Having obtained the impedance matrix of the grounding grid, the admittance matrix is calculated by the inversion of the impedance matrix. The method described in Section III is used to infer a rational fitting of the admittance matrix elements to constitute the state-space model of the grounding grid. The resultant frequency response of the grounding system is then included in EMTP-RV to calculate the lightning transient overvoltages in any location of the plant.

As for the excitation current, we consider the standard current waveform (see Fig. 11) used in EMTP-RV for modeling the first-stroke lightning current. Mathematically, the front shape of the current waveform can be expressed as [35]

$$I(t) = At + Bt^n \tag{14a}$$

and its tail shape can be defined as

$$I(t) = I_1 e^{\frac{-(t-t_n)}{t_1}} - I_2 e^{\frac{-(t-t_n)}{t_2}} \tag{14b}$$

where the time constants and current constants are dully selected to attain the typical values for waveform peak (30 kA), rise time ($1.2\,\mu$s), and fall time ($77.5\,\mu$s).

Subject to the injection of this current to the tip of the wind turbine tower (see Fig. 9), the overvoltages at different locations are calculated for both soil with constant and frequency dependent parameters. The lightning generated overvoltage at the tower footing is shown in Fig. 12 while the overvoltages at the transformer low voltage terminal (phase a) and at its neutral point are, respectively, shown in Figs. 13 and 14. From a close examination of the results in these figures, the following conclusions can be made:

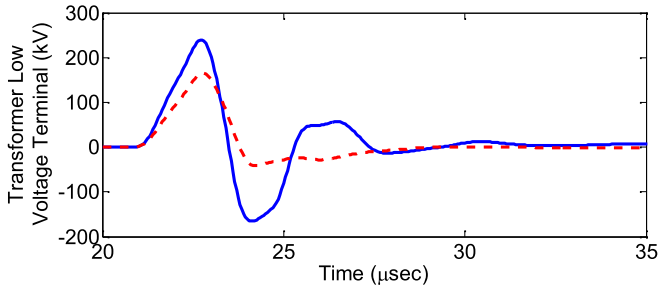

Fig. 13. Overvoltage at transformer low voltage terminal; solid line indicates soil with CPs and dashed line indicates soil with frequency-dependent parameters.

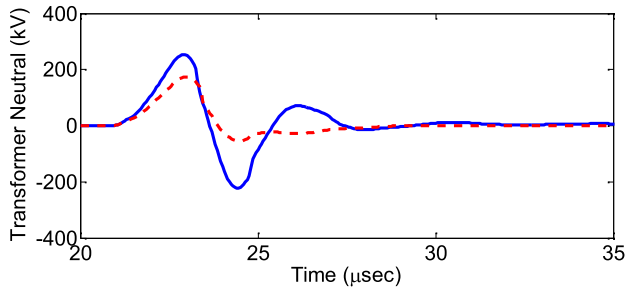

Fig. 14. Overvoltage at transformer neutral ground; solid line indicates soil with CPs and dashed line indicates soil with frequency-dependent parameters.

1) The inclusion of frequency dependence of soil electrical parameters on the grounding system modeling remarkably reduces the generated overvoltages.
2) A comparison between the rise times of the overvoltage waveforms shows that the inclusion of soil dispersion in the modeling enables one to predict the dispersive effect of wave propagation within the grounding system.

VI. Conclusion

An adaptive Chebyshev method has been proposed for expediting the calculation of grounding system admittance matrix. This helps with the characterization and the inclusion of the wideband model of the grounding systems into the time-domain electromagnetic transient solvers. The main feature of the proposed method is its ability to obtain the full response of a grounding system over the working frequency interval by applying the method of moments to the grounding system governing EFIE only at a few frequencies. The results of several simulate case studies have been presented to evaluate the performance of the proposed method. It has been shown that the adaptive Chebychev method can remarkably reduce the computation time (by reducing the frequency samples) of grounding system admittance matrix. Finally, we have used the proposed method to study the case in which lightning strikes the tip of a typical wind turbine tower, showing the noticeable effect of the frequency dependence of soil electrical parameters on the lightning-generated overvoltages.

References

[1] K. Sheshyekani, M. Akbari, B. Tabei, and R. Kazemi, "Wide band modeling of large grounding systems to interface with electromagnetic transient solvers," *IEEE Trans. Power Del.*, vol. 29, no. 4, pp. 1868–1876, Aug. 2014.
[2] M. R. Alemi and K. Sheshyekani, "Wide-band modeling of tower footing grounding system for the evaluation of lightning performance of transmission lines," *IEEE Trans. Electromagn. Compat.*, vol. 57, no. 6, pp. 1627–1636, Dec. 2015.
[3] M. Akbari, K. Sheshyekani, and M. R. Alemi, "The effect of frequency dependence of soil electrical parameters on the lightning performance of grounding systems," *IEEE Trans. Electromagn. Compat*, vol. 55, no. 4, pp. 739–746, Aug. 2013.
[4] V. Mashayekhi, S. H. H. Sadeghi, R. Moini, H. R. Karami, K. Sheshyekani, and A. Nasiri, "Frequency-dependent modeling of grounding system for wind turbine lightning transient studies," in *Proc. 2014 Int. Conf. Renew. Energy Res. Appl.*, Oct. 2014, pp. 927–931.
[5] R. Nikjoo, S. H. H. Sadeghi, and R. Moini, "A Hybrid Genetic-Simulated annealing algorithm for optimal design of grounding grids with rods," in *Proc. 2010 Asia-Pacific Power Energy Eng. Conf.*, Mar. 2010, pp. 1–4.
[6] E. Amiri, S. H. H. Sadeghi, and R. Moini, "A probabilistic approach for human safety evaluation of grounding grids in the transient regime," *IEEE Trans. Power Del.*, vol. 27, no. 2, pp. 945–952, Apr. 2012.
[7] J. C. Mason and D. C. Handscomb, *Chebyshev Polynomials*. CRC Press, Florida, USA, 2002.
[8] J. P. Boyd, "Chebyshev polynomial expansions for simultaneous approximation of two branches of a function with application to the one-dimensional Bratu equation," *Appl. Math. Comput.*, vol. 143, no. 2, pp. 89–200 2003.
[9] B. N. Datta, *Numerical linear algebra and applications*. Philadelphia, USA, Society for Industrial and Applied Mathematics (SIAM), 2010.
[10] S. Jie, T. Tang, and L.-L. Wang, *Spectral Methods: Algorithms, Analysis and Applications*, vol. 41, Springer Science & Business Media, New York, USA, 2011.
[11] T. J. Rivlin, *The Chebyshev Polynomials*, Wiley, New Jersey, USA, 1974.
[12] *Guide for Safety in AC Substation Grounding*, IEEE Std. 80-2000, 2000.
[13] A. Shoory, R. Moini, S. H. H. Sadeghi, and V. A. Rakov, "Analysis of lightning radiated electromagnetic fields in the vicinity of lossy ground," *IEEE Trans. Electromagn. Compat.*, vol. 47, no. 1, pp. 131–145, Feb. 2003.
[14] K. Sheshyekani, H. R. Karami, P. Dehkhoda, M. Paolone, and F. Rachidi, "Application of the matrix pencil method to rational fitting of frequency-domain responses," *IEEE Trans. Power Del.*, vol. 27, no. 4, pp. 2399–2408, Oct. 2012.
[15] B. Gustavsen and A. Semlyen, "Rational approximation of frequency domain responses by vector fitting," *IEEE Trans. Power Del.*, vol. 14, no. 3, pp. 1052–1061, Jul. 1999.
[16] J. H. Chung, "Efficient and physically consistent electromagnetic macromodeling of high-speed interconnects exhibiting geometric uncertainties," Ph.D. dissertation, Dept. Elect. Comput. Eng., Univ. Illinois, Urbana, IL, USA, 2012.
[17] A. V. Oppenheim, A. S. Willsky, and S. H. Nawab, *Signal and Systems, 2nd ed.* Prentice Hall, New Jersey, USA, 1997.
[18] L. Weinberg and P. Slepian, "Realizability conditions on n-port network," *Inst. Radio Eng. Trans. Circuit Theory*, vol. 5, no. 3, pp. 217–221, Sep. Oregon, USA, 1958.
[19] B. Gustavsen and A. Semlyen, "Enforcing passivity for admittance matrices approximated by rational functions," *IEEE Trans. Power Syst.*, vol. 16, no. 1, pp. 97–104, Feb. 2001.
[20] A. Borghetti, A. S. Morched, F. Napolitano, C.A. Nucci, and M. Paolone, "Lightning-Induced overvoltages transferred through distribution power transformers," *IEEE Trans. Power Del.*, vol. 24, no. 1, pp. 360–372, Jan. 2009.
[21] B. Gustavsen and A. Semlyen, "A robust approach for system identification in the frequency domain," *IEEE Trans. Power Del.*, vol. 19, no. 3, pp. 1167–1173, Jul. 2004.
[22] V. C. Silva, J. R. Cardoso, S. I. Nabeta, M. F. Palin, and F. H. Pereira, "Determination of frequency-dependent characteristics of substation grounding systems by vector finite-element analysis," *IEEE Trans. Magn.*, vol. 43, no. 4, pp. 1825–1828, Apr. 2007.
[23] *Standard for Validation of Computational Electromagnetics Computer Modeling and Simulation—Part 1, 2*, IEEE Standard P1597, 2008.

[24] A. P. Duffy, A. J. M. Martin, A Orlandi, G Antonini, T. M. Benson, and M. S. Woolfson, "Feature selective validation (FSV) for validation of computational electromagnetics (CEM). Part I—The FSV method," *IEEE Trans. Electromagn. Compat.*, vol 48, no. 3, Aug. 2006, pp 449–459.

[25] A Orlandi, A. P. Duffy, B Archambeault, G Antonini, D. E. Coleby, and S. Connor, "Feature selective validation (FSV) for validation of computational electromagnetics (CEM). Part II—Assessment of FSV performance," *IEEE Trans. Electromagn. Compat.*, vol. 48, no. 3, Aug. 2006, pp. 460–467.

[26] D. Cavka, N. Mora, and F. Rachidi, "A comparison of frequency-dependent soil models: Application to the analysis of grounding systems," *IEEE Trans. Electromagn. Compat.*, vol. 56, no. 1, pp. 177–187, Feb. 2014.

[27] K. S. Smith and C. L. Longmire, "A universal impedance for soils," *Defense Nuclear Agency*, Alexandria, VA, USA, Topical Rep., Jul. 1–Sep. 30, 1975.

[28] H. W. Dommel, *EMTP Theory Book*. Oregon, USA: Bonneville Power Administration, 1986.

[29] I. M. Dudurych, T. J. Gallagher, J. Corbett, and M. V. Escudero, "EMTP analysis of HV transmission line," *Proc. Inst. Elect. Eng., Generation, Transmission Distrib.*, vol. 150, no. 4, pp. 501–506, Jul. 2003.

[30] T. Hara and O. Yamamoto, "Modelling of a transmission tower for lightning surge analysis," *Proc. Inst. Elect. Eng., Generation, Transmission Distrib.*, vol. 143, no. 3, pp. 283–289, May 1996.

[31] IEEE Working Group 3.4.11 Surge Protective Devices Committee, "Modeling of metal oxide surge arresters," *IEEE Trans. Power Del.*, vol. 7, no. 1, pp. 302–310, Jan. 1992.

[32] A. Borghetti, A. S. Morched, F. Napolitano, C. A. Nucci, and M. Paolone, "Lightning-induced overvoltages transferred through distribution power transformers," *IEEE Trans. Power Del.*, vol. 24, no. 1, pp. 360–372, Jan. 2009.

[33] B. Badrzadeh, M. Hogdahl, and E. Isabegovic, "Transients in wind power plants—Part I: Modeling methodology and validation," in *Proc. Ind. Appl. Soc. Annu. Meeting*, Nov. 2011, pp. 1–11

[34] S. Visacro, R. Alipio, M. H. Murta Vale, and C. Pereira, "The response of grounding electrodes to lightning currents: The effect of frequency dependent soil resistivity and permittivity," *IEEE Trans. Electromagn. Compat.*, vol. 53, no. 2, pp. 401–406, May 2011.

[35] *Guide to Procedures for Estimating the Lightning Performance of Transmission Lines*, Working Group 01 (Lightning) of Study Committee 33 (Overvoltages and Insulation Co-ordination), CIGRÉ, Paris, France, Oct. 1991.

Valiollah Mashayekhi was born in Tehran, Iran, in 1983. He received the B.S. degree in electrical engineering from Shahrood University of Technology, Shahrood, Iran, in 2006, and the M.S. degree in telecommunications in 2010 from the Amirkabir University of Technology, Tehran, Iran, where he is currently working toward the Ph.D. degree.

His current research interests include electromagnetic compatibility and power system transients with particular reference to LEMP interaction with electrical networks and grounding systems.

Seyed Hossein Hesamedin Sadeghi (M'92–SM'05) received the B.S. degree in electrical engineering from the Sharif University of Technology, Tehran, Iran, in 1980, the M.S. degree in power engineering from the University of Manchester Institute of Science and Technology, Manchester, U.K., in 1984, and the Ph.D. degree in electronic systems engineering from the University of Essex, Colchester, U.K., in 1991.

In 1992, he was appointed as a Research Assistant Professor with Vanderbilt University, Nashville, TN, USA. During 1996–1997, 2005–2006, and 2012–2014, he was a Visiting Professor with the University of Wisconsin, Milwaukee, WI, USA. He is currently a Professor of Electrical Engineering with Amirkabir University of Technology, Tehran. He is the holder of four patents and is the author or coauthor of one book, one book chapter, and more than 300 scientific papers published in reviewed journals and presented at international conferences. His current research interests include electromagnetic compatibility and electromagnetic nondestructive evaluation of materials.

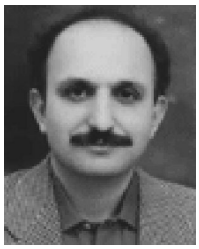

Rouzbeh Moini (M'93–SM'05) received the B.S., M.S., and Ph.D. degrees in electronics from the University of Limoges, Limoges, France, in 1984, 1985, and 1988, respectively.

In 1988, he joined the Department of Electrical Engineering, Amirkabir University of Technology, Tehran, Iran, where he is currently a Professor of Electrical Engineering. From 1995 to 1996, he was a Visiting Professor with the University of Florida, Gainesville. He is the author or coauthor of more than 250 scientific publications in reviewed journals and international conferences. His current research interests include numerical methods in electromagnetics, electromagnetic compatibility, and antenna theory.

Keyhan Sheshyekani (M'10–SM'13) received the B.S. degree in electrical engineering from Tehran University, Tehran, Iran, in 2001, and the M.S. and Ph.D. degrees in electrical engineering from Amirkabir University of Technology (Tehran Polytechnique), Tehran, Iran, in 2003 and 2008, respectively.

In September 2007, he was a Visiting Scientist with École Polytechnique, Fédérale de Lausanne Lausanne, Switzerland, where he later became a Research Assistant. From 2010 to 2015, he was an Assistant Professor with Shahid Beheshti University, Tehran, where he was an Associate Professor from 2015 to 2016. He was an Invited Professor at the EPFL from June to September 2014. In 2016, he joined the Department of Electrical Engineering, Polytechnique Montréal, Montréal, QC, Canada, where he is currently an Assistant Professor. His current research interests include power system modeling and simulation, smart grids, and electromagnetic compatibility.